Gamma-Ray Irradiation and Post-Irradiation Responses of High Dose Range RADFETs

A. Jaksic, G. Ristic, M. Pejovic, A. Mohammadzadeh, C. Sudre, and W. Lane

***Abstract*—Gamma-ray irradiation and post-irradiation responses have been studied for the two types of radiation sensitive p-channel MOSFETs (RADFETs) from different manufacturers. In addition to, in dosimetric applications standard, threshold voltage measurements at a single specified current, transistor I–V and charge-pumping characteristics have been monitored. This has been shown to be useful in providing a more detailed insight into processes that occur during irradiation and subsequent annealing at elevated temperature. In particular, the role of switching oxide traps (also known as "border" traps) and electron traps in studied devices has been revealed.**

***Index Terms*—Characterization, RADFET, radiation dosimeters.**

I. Introduction

SINCE the introduction of the space-charge dosimeter concept [1], radiation sensitive p-channel MOSFETs (also known as RADFETs) have been developed for applications such as space, nuclear industry and research, and radiotherapy [1]–[4]. Other types of dosimeters that are commonly used or are being developed for these applications include thermoluminescent dosimeters (TLDs), semiconductor diodes, and optically stimulated luminescence dosimeters (OSDLs). A comprehensive review of radiation dosimetry issues and devices can be found in [5]. The TLDs are rather small, well characterized, and standard in use, however, they are not suitable for remote measurements and the readout of dosimetric information is destructive. Semiconductor diodes are also miniature in size, but produce small dosimetric signal and require high voltage. The optically stimulated luminescenc (OSL) dosimetry concept has re-emerged recently with promising results [6], [7], however, OSLDs require integration of electronics and optic elements in the readout system and dosimetric information is read destructively. The RADFET advantages include immediate, nondestructive readout of dosimetric information, extremely small size, very low power consumption, all-electronic interfaces fully compatible with microprocessors, high dose range, and very competitive price. The RADFET disadvantages are a need for calibration in different radiation fields, relatively low resolution (starting from about 1 rad), and nonreusability. A new design approach has been investigated recently that could overcome the low resolution problem and introduce the RADFETs into the personnel dosimetry area ([8] and references therein).

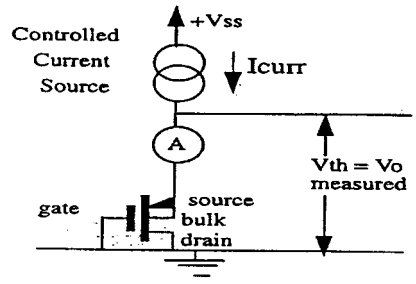

Fig. 1. Reader circuit (RC) configuration for threshold-voltage measurements in RADFETs; $I\mathrm{curr} = 10\mu\mathrm{A}$ was used.

The NMRC have been active in RADFET research and development since the late 1980s, resulting in a range of commercially available RADFETs for various applications [9], i.e., different dose ranges. This paper will present and discuss the irradiation and post-irradiation response of low sensitivity/high dose range RADFETs. These RADFETs typically have about 100-nm-thick gate oxides (gate oxide of high sensitivity/low dose range RADFETs can be up to 1 μm thick) and are suitable for space and nuclear research/industry applications. We will examine the RADFET response in the space dose range, i.e., up to the total absorbed doses of several hundred Gy (1 Gy $=$ 100 rad). The responses of devices from two different manufacturers will be compared.

Radiation induces charge trapping in the gate oxide and at the Si/SiO_2 interface, causing the threshold voltage shift (ΔV_T), which is the RADFET dosimetric parameter. There are several definitions of the MOSFET threshold voltage (V_T) [10], however the one that is most commonly used in RADFET applications is that the V_T is the voltage needed to sustain a specified current. Thus, the V_T is measured at a single point of the transfer I–V characteristics, applying a specified current (typically in the order of 10 μA) to the RADFET in two-terminal mode (source and bulk are shorted and represent one terminal, while drain and gate are also shorted and represent another terminal). This configuration will be referred to as a reader circuit (RC) configuration and is shown in Fig. 1. While, for its

Manuscript received October 8, 2001; revised March 11, 2002.

A. Jaksic is with the National Microelectronics Research Centre (NMRC), Cork, Ireland (e-mail: ajaksic@nmrc.ie).

G. Ristic is with the Sunnybrook Health Science Center, University of Toronto, Toronto, ON M4N 3M5 Canada (e-mail: gristic@sten.sunnybrook.utoronto.ca).

M. Pejovic is with the Faculty of Electronic Engineering, University of Nis, Yugoslavia (e-mail: pejovic@elfak.ni.ac.yu).

A. Mohammadzadeh is with the European Space Agency (ESA/ESTEC), Noordwijk, The Netherlands (e-mail: ali.mohammadzadeh@esa.int).

C. Sudre was with the National Microelectronics Research Centre, Cork, Ireland. He is now with General Semiconductors, Freiburg, Germany (e-mail: csudre@gensemi.com).

W. Lane was with the National Microelectronics Research Centre, Cork, Ireland. He is now with Analog Devices, Cork, Ireland (e-mail: bill.lane@analog.com).

Publisher Item Identifier S 0018-9499(02)05823-9.

simplicity, the RC configuration is suitable for practical applications and calibration measurements, it does not provide the quantification of and insight into the charge-trapping mechanisms that could serve as the basis for RADFET fabrication process improvements. For this reason, we have performed I–V and charge-pumping (CP) measurements in addition to the RC measurements. This has enabled us to analyze basic mechanisms underlying irradiation and post-irradiation behaviors of the RADFETs and, in particular, discuss the role of switching oxide traps in studied devices.

II. Experimental Details

The RADFETs from two different manufacturers (NMRC, Ireland, and EI-Microelectronics, Yugoslavia) have been investigated. Both types of devices are p-channel MOSFETs fabricated in Al-gate process. The NMRC RADFETs have 100-nm-thick gate oxide, grown at 1000 °C in dry oxygen, and annealed for 15 min at 1000 °C in nitrogen. The post-metallization anneal (PMA) was performed at 440 °C in forming gas for 60 min. The EI RADFETs ([11] and references therein) have 110-nm-thick gate oxide, grown at 1150 °C in wet oxygen, and annealed for 60 min at 1050 °C in nitrogen. The 30-min PMA was done at 440 °C in forming gas.

Experimental samples were irradiated at room temperature using the Co-60 source to 300 Gy at the dose rate of 0.013 Gy/s. All doses are given in Gy(H_2O), to convert to Gy(SiO_2) $\approx$ Gy(Si), one has to multiply the dose by 0.898. The gate bias during irradiation ($V_{\rm irr}$) was either 0 or +5 V. Immediately after irradiation, the devices were annealed at 100 °C with −10-, 0-, or +10-V annealing bias ($V_{\rm ann}$). There were at least two (and in many cases more) samples for each annealing experimental condition in terms of $V_{\rm irr}/V_{\rm ann}$ values. The discrepancies between nominally identical samples were in all cases within 5%. The V_T values were determined using the RC configuration with 10-μA current (Fig. 1). In addition, device transfer I–V characteristics in saturation were recorded, enabling determination of the "extrapolated" V_T and channel mobility (μ) [10]. The densities of radiation-induced fixed traps ($\Delta N_{\rm ft}$[cm^{-2}]) and switching traps ($\Delta N_{\rm st}$[cm^{-2}]) were determined from the sub-threshold I–V curves using the midgap technique (MGT) of McWhorter and Winokur [12]. Finally, the charge-pumping technique (CPT) measurements [13] were performed to determine the energetic densities of switching traps ($\Delta D_{\rm st}$[cm^{-2}eV^{-1}]), $\Delta N_{\rm st} = \Delta D_{\rm st} \times \Delta E$, where ΔE[eV] is an energy range within the Si bandgap scanned by the measurement. Parameters of the CP measurements (recording of Elliot-type CP curves [14], triangular pulse, frequency 100 kHz, amplitude 4 V, duty cycle 50%) were such that CPT and MGT scanned regions within the silicon bandgap of the same energetic widths (approx. 0.43 eV). Thus, the $\Delta N_{\rm st}$ values obtained by MGT and CPT will be directly compared in this paper.

Note that the terms "fixed" and "switching" are used here to define the electrical response of the traps: while fixed traps do not exchange charge with the Si during the time frame of the measurement, switching traps do. Thus, fixed traps cause parallel shift in subthreshold transfer I–V characteristics (MGT) or Elliot-type CP curves (CPT). Switching traps result in an increase of the subthreshold slope (MGT) or of the CP current (CPT). As to the location of these traps, fixed traps are located exclusively in the oxide, while switching traps can be exactly at the Si/SiO_2 interface (interface traps, density ΔN[cm^{-2}]) or in near-interfacial region of the oxide (switching oxide traps, also known as border traps [15], density $\Delta N_{\rm sot}$[cm^{-2}]). Thus, the oxide traps include fixed oxide traps and switching oxide traps, and their total density can be expressed as $\Delta N_{\rm ot} = \Delta N_{\rm ft} + \Delta N_{\rm sot}$. The aforementioned nomenclature was adopted as it better suits the nature of measurements that were done on the experimental samples. Namely, both MG and CP are electrical measurements that can distinguish the radiation-induced defects by their electrical response rather than by location. More details on this will follow in Section III.

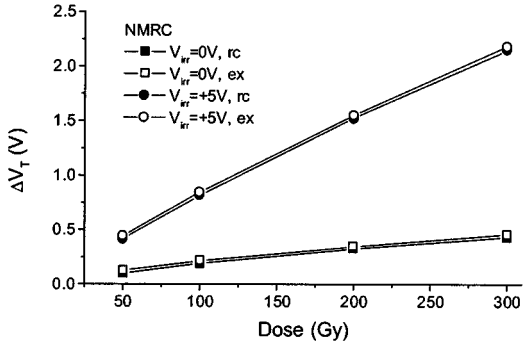

Fig. 2. NMRC samples: reader circuit (rc) and extrapolated (ex) ΔV_T during irradiation with zero and positive gate bias.

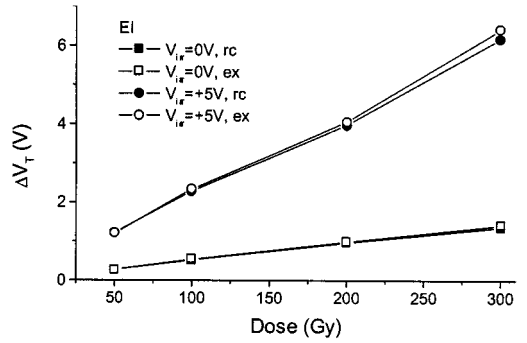

Fig. 3. EI samples: rc and ex ΔV_T during irradiation with zero and positive gate bias.

III. Results and Discussion

A. Irradiation

Figs. 2 and 3 show extrapolated and reader circuit ΔV_T during irradiation for NMRC and EI samples, respectively. The agreement between extrapolated and reader circuit ΔV_T is very good (within 1–2%) in all cases, justifying the use of the RC configuration in practical applications. The radiation sensitivities determined at 300 Gy are given in Table I.

The EI samples have roughly a factor of 3 higher sensitivity for both $V_{\rm irr}$ conditions. Only a small fraction of the difference can be attributed to somewhat greater oxide thickness of the EI samples (110 nm versus 100 nm in the NMRC samples). By

TABLE I
NMRC AND EI SAMPLES: SENSITIVITY FIGURES ([mV/cGy] AT 300 Gy(H_2O))

	V_{irr}=0V	V_{irr}=+5V
NMRC	0.015	0.071
EI	0.047	0.217

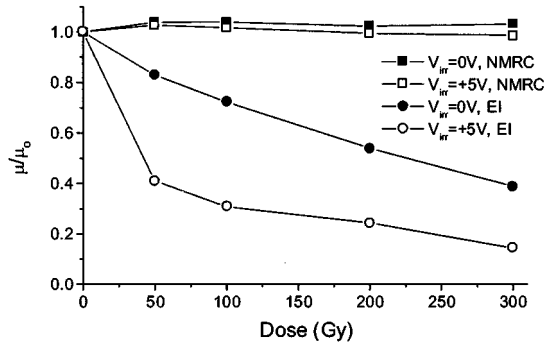

Fig. 4. NMRC and EI samples: μ/μ_o during irradiation with zero and positive gate bias.

far, the most of the sensitivity difference comes from charge trapping properties of EI RADFET gate oxide (more details to follow). Note that the high sensitivity may not necessarily be an advantage, particularly in very high dose applications, as it will reduce the maximum detectable dose [2].

Fig. 4 shows the changes in μ, normalized to pre-irradiation value (μ_o), during irradiation. There is almost no change in μ in NMRC samples, while there is a large μ decrease, enhanced by positive $V_{\rm irr}$ in EI samples.

Figs. 5 and 6 show $\Delta N_{\rm ft}$ and $\Delta N_{\rm st}$ during irradiation for NMRC and EI samples, respectively. As expected, positive $V_{\rm irr}$ enhances formation of both fixed and switching traps. The MGT and CPT data are in qualitative agreement, but the $\Delta N_{\rm st}$(CPT) is in all cases lower than $\Delta N_{\rm st}$(MGT). The exact quantitative agreement should not be expected for at least two reasons. First, the two techniques have different effective frequencies: a few hertz (MGT) versus 100 kHz (CPT). Both MGT and CPT are capable of sensing the interface traps, which are very fast, but the contributions of switching oxide traps to the CP and MG signals are not the same. While MGT senses almost all switching oxide traps (slow, medium fast, and fast), the CP signal in our case excludes at least contributions of slow and medium fast switching oxide traps, and, consequently, $\Delta N_{\rm st}$(CPT) is expected to be lower. Second, the two techniques scan different portions of the Si bandgap: lower half (MGT) versus central portion (CPT). As interface traps have a U-shaped distribution toward the edges of the bandgap [10], [16] and that portion cannot be reached by CPT, this is an additional reason that may lead to the lower $\Delta N_{\rm st}$(CPT) values. The $\Delta N_{\rm ft}$ dominates in NMRC samples (at 300 Gy, $\Delta N_{\rm ft}/\Delta N_{\rm st}$ equals 1.9 for $V_{\rm irr} = 0$ V, and 3.7 for $V_{\rm irr} = +5$ V). However, in EI samples, $\Delta N_{\rm st}$(MGT) even exceeds $\Delta N_{\rm ft}$. Thus, the greater sensitivity of EI samples is mostly due to the enhanced formation of switching traps (i.e., switching oxide traps and interface traps). It is probable that some portion (NMRC samples) or even most of the $\Delta N_{\rm ft}$ determined by MGT (EI samples) is due to switching oxide traps [17] (see later discussion).

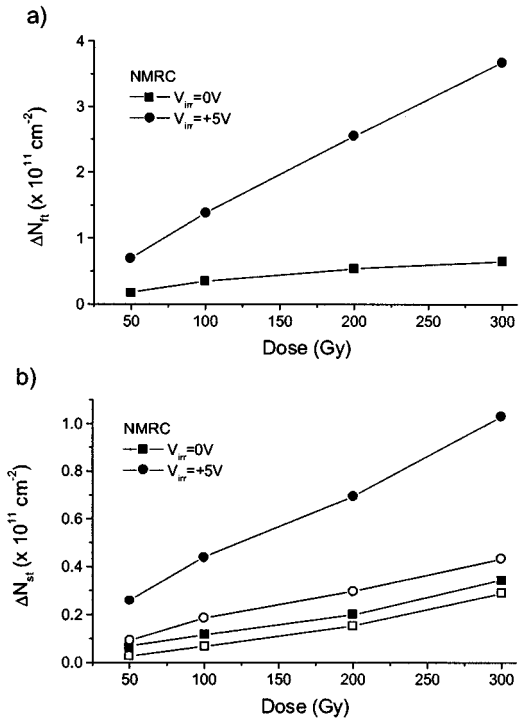

Fig. 5. NMRC samples. (a) $\Delta N_{\rm ft}$ and (b) $\Delta N_{\rm st}$ (MG-solid symbols, CP-open symbols) during irradiation with zero and positive gate bias.

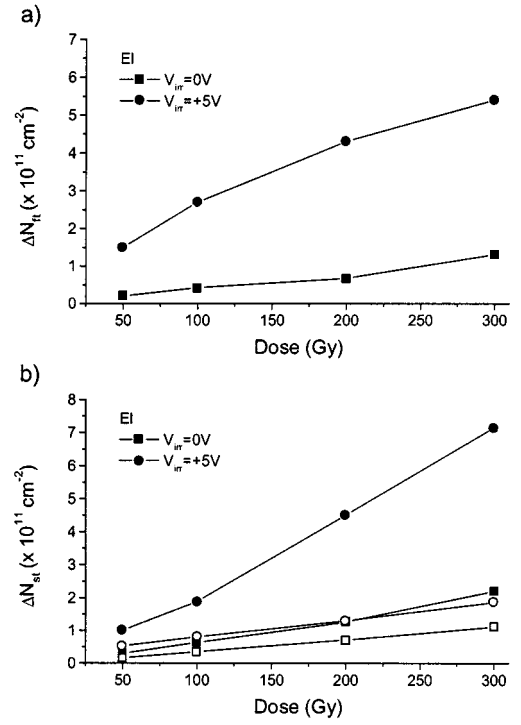

Fig. 6. EI samples. (a) $\Delta N_{\rm ft}$ and (b) $\Delta N_{\rm st}$ (MG-solid symbols, CP-open symbols) during irradiation with zero and positive gate bias.

The CPT provides means for estimating not only $\Delta N_{\rm st}$, but also the absolute switching trap densities $(N_{\rm st})$. The pre-irradiation $N_{\rm st}$ values are $(1.18 \pm 0.03) \times 10^{10}$ cm^{-2}eV^{-1} in NMRC samples, and $(0.42 \pm 0.09) \times 10^{10}$ cm^{-2}eV^{-1} in EI samples.While pre-irradiation $N_{\rm st}$ is higher in the NMRC samples, the fabrication process is better controlled in this respect than

the EI one, with much lower $N_{\rm st}$ variations between the samples. The range of $N_{\rm st}$ increase after irradiation in NMRC samples is 4–5 times, while in EI samples it is 30–50 times.

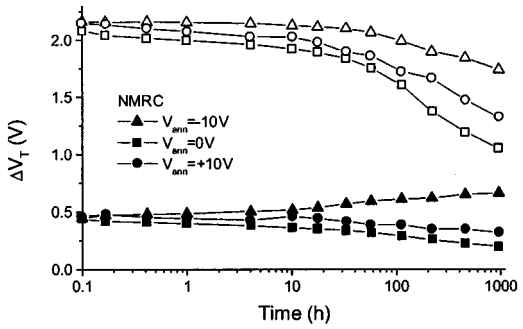

Fig. 7. NMRC samples. ΔV_T during annealing at 100 °C with negative, zero, and positive gate bias; solid symbols—zero irradiation bias, open symbols—positive irradiation bias (+5 V).

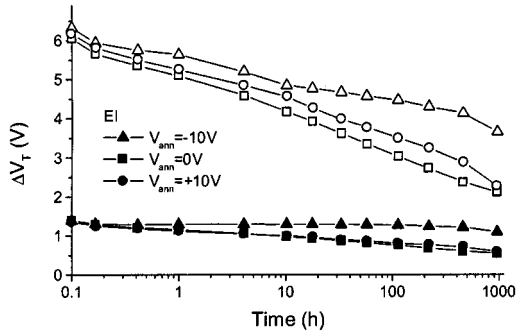

Fig. 8. EI samples. ΔV_T during annealing at 100 °C with negative, zero, and positive gate bias; solid symbols—zero irradiation bias, open symbols—positive irradiation bias (+5 V).

B. Annealing

Figs. 7 and 8 show ΔV_T evolution during annealing for NMRC and EI samples, respectively. The ΔV_T behavior depends primarily on $V_{\rm ann}$. It is interesting to note that in both samples, the loss of dosimetric information (fading) is more pronounced for zero than for positive $V_{\rm ann}$.

The μ/μ_o evolution during annealing is shown in Figs. 9 and 10. One of the intentions of our study was to determine the effect of fixed oxide traps on μ in p-channel MOSFETs. Namely, it has been unambiguously established that interface traps have predominant effect on μ, acting to decrease μ in both n- and p-channel devices [18], [19]. The effect of fixed oxide traps in n-channel devices is qualitatively the same, although quantitatively less pronounced. However, there is still some uncertainty as to whether fixed oxide traps act to decrease or increase μ in p-channel devices. The former is argued by Zupac *et al.* ([20] and references therein) and has been observed by others as well [21], [22]. The latter has been demonstrated by Dimitrijev and Stojadinovic *et al.* [23] and attributed to decreased surface-roughness scattering in the presence of fixed oxide traps. In order to confirm one of these models, one has to study p-channel devices in which interface trap creation is negligible in comparison with fixed oxide trap creation. Unfortunately, as the $\Delta N_{\rm ft}/\Delta N_{\rm st}$ ratio is found to be (unexpectedly)

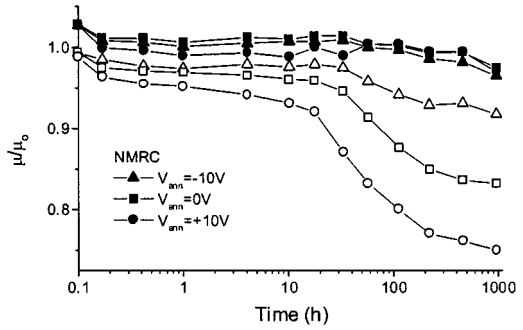

Fig. 9. NMRC samples: μ/μ_o during annealing at 100 °C with negative, zero, and positive gate bias; solid symbols—zero irradiation bias, open symbols—positive irradiation bias (+5 V).

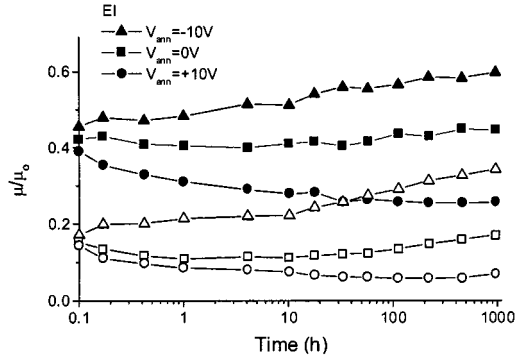

Fig. 10. EI samples: μ/μ_o during annealing at 100 °C with negative, zero, and positive gate bias; solid symbols—zero irradiation bias, open symbols—positive irradiation bias (+5 V).

low in both types of RADFETs studied here, the predominant effect of $\Delta N_{\rm st}$ obscures the effect of $\Delta N_{\rm ft}$. In addition, the contribution of switching oxide traps to $\Delta N_{\rm st}$ complicates even quantification of the effects of interface traps on μ. Consequently, no conclusion about $\Delta N_{\rm ft}$ effects on μ can be made based on the obtained data. Indeed, it can be seen in Figs. 9 and 10 that μ generally follows the pattern of inverse $\Delta N_{\rm st}$ [$\Delta N_{\rm st}$ is shown in Figs. 11(b)–14(b)].

Figs. 11 and 12 show $\Delta N_{\rm ft}$ and $\Delta N_{\rm st}$ during annealing for NMRC samples for the case of zero and positive $V_{\rm irr}$, respectively. The positive $V_{\rm ann}$ enhances formation of switching traps and decay of fixed traps. The $\Delta N_{\rm ft}$ even goes into the negative region, particularly in $V_{\rm irr} = 0$ V case. Note that there is still a qualitative agreement between $\Delta N_{\rm st}$ values obtained by CPT and MGT. Moreover, the changes in $\Delta N_{\rm st}$ during annealing as determined by the two techniques are roughly the same.

Finally, Figs. 13 and 14 show the same data as Figs. 11 and 12, but for EI samples. The $\Delta N_{\rm ft}$ pattern is qualitatively similar to that in NMRC samples (positive $V_{\rm ann}$ enhances the decrease of $\Delta N_{\rm ft}$). However, there are some quantitative differences, such as larger magnitude of negative $\Delta N_{\rm ft}$ observed for both $V_{\rm irr} = 0$ and +5 V, particularly in the case of $V_{\rm ann} = +10$ V. As to $\Delta N_{\rm st}$, opposite to the pattern observed in NMRC samples, there is even an absence of $\Delta N_{\rm st}$(MGT) and $\Delta N_{\rm st}$(CPT) qualitative agreement, again particularly for $V_{\rm ann} = +10$ V. Generally, $\Delta N_{\rm st}$(CPT) stays little changed, while $\Delta N_{\rm st}$(MGT) increases substantially ($V_{\rm ann} = +10$ V) or decreases (e.g., $V_{\rm irr} = +0$ V, $V_{\rm ann} = -10$ V in Fig. 13(b).

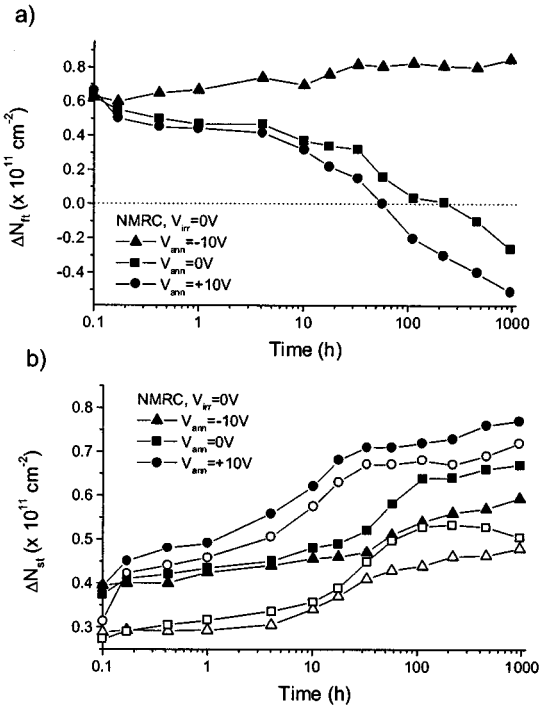

Fig. 11. NMRC samples. (a) $\Delta N_{\rm ft}$ and (b) $\Delta N_{\rm st}$ (MG-solid symbols, CP-open symbols) during annealing at 100 °C with negative, zero, and positive gate bias; zero irradiation bias.

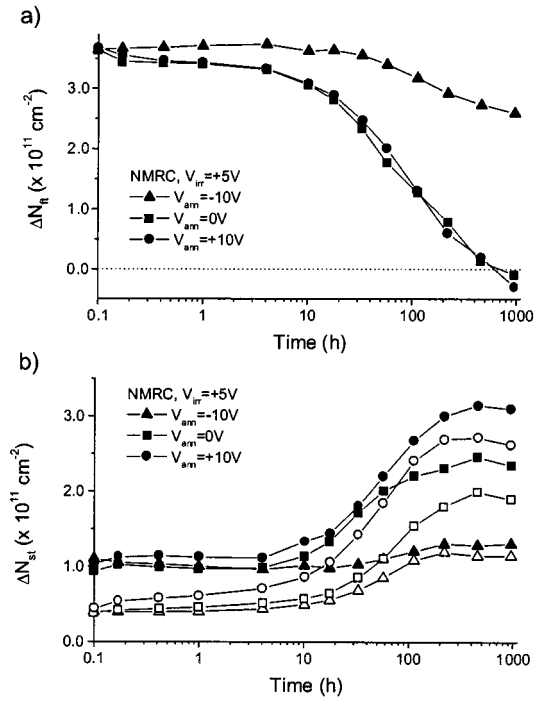

Fig. 12. NMRC samples. (a) $\Delta N_{\rm ft}$ and (b) $\Delta N_{\rm st}$ (MG-solid symbols, CP-open symbols) during annealing at 100 °C with negative, zero, and positive gate bias; positive irradiation bias (+5 V).

C. Microscopic Mechanisms

Presented experimental results can be most readily explained within the general context of the HDL model [24]–[26]. The crucial role in this model belongs to the E'_γ center, which is a weak Si–Si bond in the oxide caused by an oxygen atom vacancy between two Si atoms, each back-bonded to three oxygen atoms [27]. The E'_γ center acts as a hole trap and is predominantly responsible for the increase of oxide trapped charge during irradia-

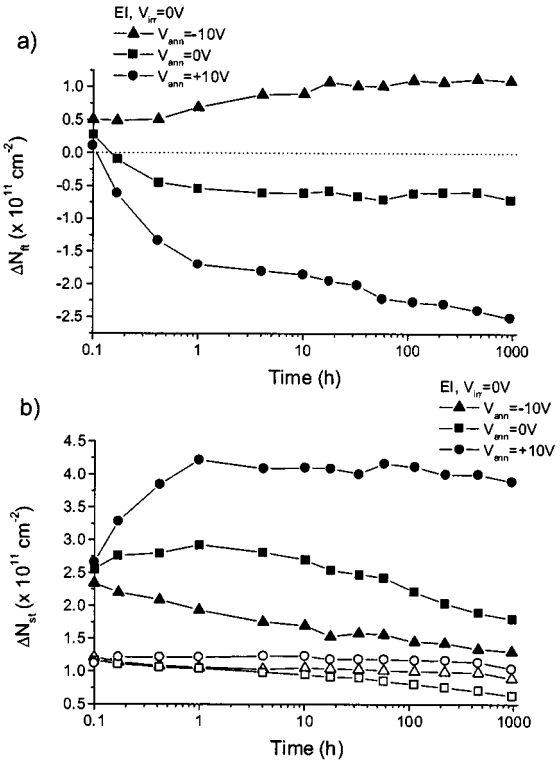

Fig. 13. EI samples. (a) $\Delta N_{\rm ft}$ and (b) $\Delta N_{\rm st}$ (MG-solid symbols, CP-open symbols) during annealing at 100 °C with negative, zero, and positive gate bias; zero irradiation bias.

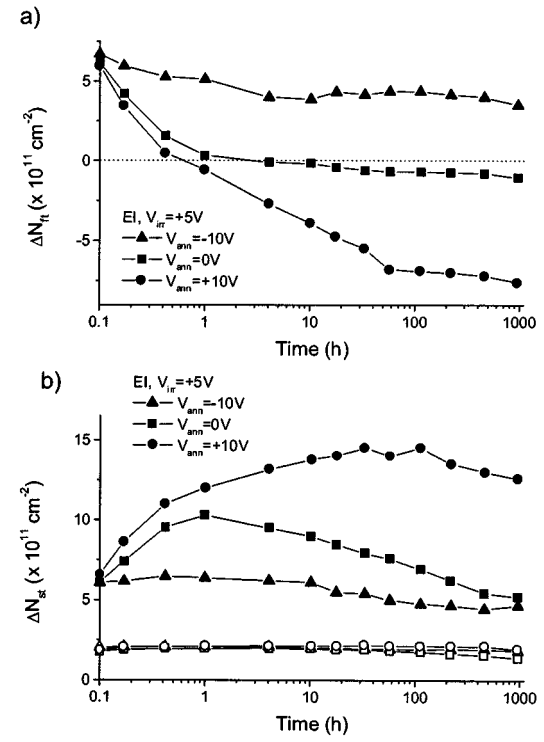

Fig. 14. EI samples. (a) $\Delta N_{\rm ft}$ and (b) $\Delta N_{\rm st}$ (MG-solid symbols, CP-open symbols) during annealing at 100 °C with negative, zero. and positive gate bias; positive irradiation bias (+5 V).

tion [28]. As discussed in Section II, the oxide trapped charge involves both charge trapped at fixed oxide traps and that trapped at switching oxide traps. Namely, under the influence of the positive electric field in the oxide (caused by positive gate bias) during annealing, the hole trapped at the E'_γ center can be either compensated or neutralized by the electron tunneling from Si. In the case of compensation, when the negative field (negative gate bias) is applied, the electron can tunnel back to Si, leaving the E'_γ center positively charged. Thus, some of the E'_γ centers can communicate electrically with Si, the communication being easier and faster in case they are closer to the Si/SiO_2 interface. We will accept convincing arguments of Lelis and Oldham [26] that the switching oxide traps in irradiated oxides are E'_γ centers close to the Si/SiO_2 interface. The fixed oxide traps are microscopically E'_γ centers as well, however further from the Si/SiO_2 interface and hence incapable of exchanging charge with Si during the time frame of the measurements.

The negative $\Delta N_{\rm ft}$ observed at certain bias conditions in both NMRC and EI samples indicates that there is also negative charge, i.e., electron trapping in the oxide. Such phenomenon has been observed previously in MOSFET oxides and its importance in radiation response demonstrated [29]–[32]. Electron trapping can also be attributed to E'_γ centers [26]. Namely, it has been proposed [33], [26] that, under appropriate conditions, the compensated E'_γ center can capture a second electron and become net negative. In other words, after electron capture, E'_γ center becomes an amphoteric trap that can either release or capture an electron and become positively or negatively charged, respectively.

As discussed in Section II, the MGT is a slow technique that registers both interface traps and near-interfacial switching oxide traps (E'_γ centers) as switching traps. The much faster CPT registers as switching traps the interface traps and perhaps only the fastest switching oxide traps, i.e., the E'_γ centers closest to the Si/SiO_2 interface that cannot be distinguished from interface traps. Thus, the CPT can be used for at least rough estimation of the interface trap behavior, and combination of MGT and CPT in some cases may provide information about switching oxide traps.

It is clear that $\Delta N_{\rm ft}$, $\Delta N_{\rm sot}$, and $\Delta N_{\rm it}$ all increase during irradiation. The exact proportion between $\Delta N_{\rm sot}$ and $\Delta N_{\rm it}$ during irradiation is difficult to determine, but it is probable that a significant part of $\Delta N_{\rm st}$ in NMRC samples and dominant part of $\Delta N_{\rm st}$ in EI samples is due to switching oxide traps. This would be in line with observations of Fleetwood *et al.* [17] in soft oxides.

The $\Delta N_{\rm ft}$ behavior during annealing [Figs. 11(a)–14(a)] is consistent with the HDL model. For example, for $V_{\rm ann} = -10$ V, $\Delta N_{\rm ft}$ increases ($V_{\rm irr} = 0$ V) or decreases slightly ($V_{\rm irr} = +5$ V) in both NMRC and EI samples. The increase for $V_{\rm irr} = 0$ V is due to tunneling of trapped holes from E'_γ centers to Si under the influence of negative electric field at the Si/SiO_2 interface. The slight decrease for $V_{\rm irr} = +5$ V indicates that the built-in positive field in the vicinity of the interface due to radiation-induced positive charge is stronger than the negative filed caused by $V_{\rm ann}$, enabling the electrons to tunnel from Si to E'_γ centers and neutralize the holes trapped there. As expected, much more pronounced $\Delta N_{\rm ft}$ decrease is observed for $V_{\rm ann} = 0$ and $+10$ V, which both correspond to the positive electric field at the Si/SiO_2 interface, the field being greater in magnitude in the latter case and hence $\Delta N_{\rm ft}$ decrease being enhanced. Besides neutralization of charge trapped at E'_γ centers by electrons tunneling from Si under the influence of electric field, the electrons thermally emitted from the oxide valence band also contribute to E'_γ centers neutralization [34]. Finally, electron trapping is another mechanism causing $\Delta N_{\rm ft}$ decrease. Electron trapping is more pronounced in EI samples, and, as expected, for positive $V_{\rm ann}$.

TABLE II
NMRC AND EI SAMPLES: $\Delta N_{\rm ft}$, $\Delta N_{\rm sot}$, AND $\Delta N_{\rm it}$ PATTERNS DURING ANNEALING WITH $V_{\rm ann} = +10$ V

	ΔN_{ft}	ΔN_{it}	ΔN_{sot}
NMRC	↓	↑	↔
EI	↓	↔	↑

If we consider $\Delta N_{\rm st}$ behavior during annealing [Figs. 11(b)–14(b)], in NMRC samples there is $\Delta N_{\rm st}$(MGT) increase closely followed by $\Delta N_{\rm st}$(CPT) increase. The parallel offset between $\Delta N_{\rm st}$(MGT) and $\Delta N_{\rm st}$(CPT) implies that there is a genuine increase in interface traps during annealing and that the number of switching oxide traps stays roughly unchanged. This is consistent with previous results by Fleetwood *et al.* [17]. The buildup of interface traps during irradiation and annealing can be explained by the so-called hydrogen models [16], which involve release of hydrogenous species (H^+ ions [35] and/or H_2 molecules [36]) in the oxide, their transport to the Si/SiO_2 interface and reactions in which interface traps are formed. According to hydrogen models, details of interface traps behavior are determined by the hydrogen content of the oxide and $V_{\rm ann}$ (both increased hydrogen content and positive $V_{\rm ann}$ enhance formation of interface traps). Interface trap models will not be elaborated in detail here, the reader is referred to the original work ([35], [36], and references therein).

In EI samples, $\Delta N_{\rm st}$(CPT) is roughly constant during annealing, implying that there is little or no change in $\Delta N_{\rm it}$, and, hence, $\Delta N_{\rm st}$(MGT) behavior approximates that of $\Delta N_{\rm sot}$. For $V_{\rm ann} = +10$ V, similar to NMRC samples, there is a substantial increase in $\Delta N_{\rm st}$(MGT). However, in contrast to NMRC samples, $\Delta N_{\rm st}$(MGT) increase is due to switching oxide traps, and not interface traps. The patterns of $\Delta N_{\rm ft}$, $\Delta N_{\rm sot}$, and $\Delta N_{\rm it}$ behaviors during annealing with $V_{\rm ann} = +10$ V are summarized in Table II.

For $V_{\rm ann} = -10$ V, there is a decrease in $\Delta N_{\rm st}$(MGT). The decrease is more pronounced in the case of $V_{\rm irr} = 0$ V than $V_{\rm irr} = +5$ V, most probably because the resultant field at the Si/SiO_2 interface is more negative in the former case owing to less positive charge trapped [compare $\Delta N_{\rm ft}$ in Figs. 13(a) and 14(a)]. For an intermediate case of $V_{\rm ann} = 0$ V, an initial increase in $\Delta N_{\rm st}$(MGT) is followed by a decrease at later annealing times. The turn-around point is at the time when the electric field at the Si/SiO_2 interface, primarily determined by the sign of $\Delta N_{\rm ft}$, turns negative [see, e.g., Fig. 14(b)]. It seems that in EI samples the electric field at the interface determines switching oxide traps behavior: the positive field acts to increase $\Delta N_{\rm sot}$, while the negative field acts to decrease $\Delta N_{\rm sot}$. This can be explained by assuming that tunneling of electrons from

Si to the E'_γ centers under the positive bias results in creation of switching oxide traps. On the other hand, tunneling of electrons from E'_γ centers to Si leaves the centers in the state in which they cannot exchange charge with Si during the measurements. Microscopically, all these defects are related to the E'_γ centers, but the capture or release of electron changes the energy level and thereby the nature of the center. Physical location of the centers and their energy levels may differ from oxide to oxide, causing different radiation responses as observed in our study.

D. Effects of Processing Steps

Differences in details of the radiation response of NMRC and EI samples (see, e.g., Table II) are the consequence of different parameters of processing steps used during fabrication of experimental samples. It is not easy to unambiguously determine which particular process step is crucial for the explanation of the radiation response, as the response is often determined not only by the individual step, but by the process sequence within which it occurs [16]. Nevertheless, general impact of certain steps has been documented and can be analyzed.

As E'_γ centers are argued to have a dominant role in hole and electron trapping at both fixed or switching traps in the oxides investigated here, we will discuss the process steps crucial for E'_γ centers formation. It has been shown [37] that the formation of E'_γ centers is predominantly affected by the highest temperature used in the process flow. In our case of Al-gate devices it is the oxidation temperature. In addition, the post-oxidation anneal (POA) step has been shown to be of the most importance for the switching oxide trap behavior. Both oxidation and POA were performed at higher temperatures in EI samples, and the POA duration was longer as well. Increased oxidation temperature, POA temperature, and POA duration all act to increase the number of E'_γ centers in the oxide [38], [39]. This may be the explanation for higher radiation sensitivity due to increased charge trapping in EI samples, as well as for generally more pronounced changes in $\Delta N_{\rm ft}$ and $\Delta N_{\rm st}$ during annealing. On the other hand, it has been argued [37]–[39] that the higher temperature POA relieves the strain in the vicinity of the Si/SiO_2 interface. Within the context of DHL model, relieved strain leads to the smaller number of E'_γ centers that act as switching oxide traps, while it does not necessarily mean smaller total number of E'_γ centers [26], [40]. Such oxides would exhibit slower decay of $\Delta N_{\rm ft}$ during annealing [40], which is not observed in our case. Perhaps the reason for this discrepancy is in the complex influence of not only individual process steps but also certain process sequences on location and energy levels of the traps in the oxide. The problem is also in the inability of the employed characterization techniques to provide information about some pertinent details of the microscopic processes that occur during irradiation and annealing. For example, it still cannot be distinguished by CPT with complete certainty whether the $\Delta N_{\rm it}$ increase in NMRC samples [Figs. 11(b) and 12(b)] is really entirely due to interface traps or to switching oxide traps very near the Si/SiO_2 interface. Similarly, the effects of hole and electron trapping are both contained in $\Delta N_{\rm ft}$ data and cannot be separated using MGT. In addition, the MGT can be sensitive to lateral nonuniformities (LNUs) in the trapped charge distribution in the oxide [41], which may further complicate precise quantification of the $\Delta N_{\rm st}$ contribution.

IV. Conclusion

Radiation and post-irradiation responses of the two types of low sensitivity/high dose range RADFETs have been investigated. Measurements in practical applications and during RADFET calibration typically involve determination of the threshold voltage only in a single specified point of the device I–V characteristic. While such procedure is confirmed to be sufficient from the application point of view, RADFET further development requires insight into microscopic processes that occur during irradiation and subsequent annealing. This study has demonstrated the use of subthreshold midgap and charge-pumping techniques in RADFETs. Admittedly, these electrical techniques have limitations, such as that they cannot provide information of the microscopic structure of the defects in the oxide and at the Si/SiO_2 interface, cannot clearly distinguish the contributions of electrons and holes to the charge trapped in the oxide, or are sensitive to LNUs (MGT). However, concurrent use of MGT and CPT can still provide valuable information about the effects of switching oxide traps and interface traps, which are indistinguishable when a single technique (e.g., MGT) is used. The knowledge about behavior patterns of interface traps, switching oxide traps, together with that of fixed oxide traps, is crucial in optimizing the RADFET response. Often complex interplay between these three types of traps determines radiation sensitivity and post-irradiation stability (fading). That explains, for instance, the somewhat unexpected result in Figs. 7 and 8 that fading is lower for $V_{\rm ann} = +10$ V than for $V_{\rm ann} = 0$ V. (It is expected that the fading for $V_{\rm ann} = -10$ V is the lowest.) Switching oxide traps are particularly important in RADFETs as they have the dominant influence on another important parameter—a short-term drift [42].

It has been proposed that the E'_γ centers play a crucial role in RADFET response, being responsible for both fixed and switching traps in the oxide and for both hole and electron trapping. Therefore, the need to optimize the RADFET fabrication process in terms of E'_γ centers number, location, and energy is of paramount importance. This can be done by optimization of the highest temperature processes, i.e., usually gate oxidation and subsequent anneal in an inert atmosphere. However, one should be careful when making conclusions because sometimes the whole process sequence rather than individual process steps can have an impact on radiation and post-irradiation response of the devices.

Another approach to optimizing the RADFET response would be the use of oxide–nitride structures instead of standard, thermal gate oxides [43], [44]. These RADFETs operate with negative bias applied on the gate, and the charge trapping does not occur at the Si/SiO_2 interface, but at the SiO_2/Si_3N_4 interface. The role of electron tunneling, and, consequently, E'_γ centers, is not crucial in these devices, and they should exhibit superior fading and drift characteristics [43], [44]. However, as the charge is trapped further from the Si/SiO_2 interface, such RADFETs would in general be less sensitive, limiting their use to high dose applications with stringent fading requirements.

REFERENCES

[1] A. Holmes-Siedle, "The space-charge dosimeter," *Nucl. Instrum. Methods*, vol. 121, pp. 169–179, 1974.

[2] A. Holmes-Siedle and L. Adams, "RADFET: A review of the use of metal–oxide–silicon devices as integrating dosimeters," *Radiat. Phys. Chem.*, vol. 28, pp. 235–244, 1986.

[3] A. Kelleher, N. McDonnell, B. O'Neill, L. Adams, and W. Lane, "The effect of gate oxide process variations on the long-term fading of the PMOS dosimeters," *Sensors Actuators A*, vol. 37–38, pp. 370–374, 1993.

[4] D. J. Gladstone, X. Q. Lu, J. L. Humm, H. F. Bowman, and L. M. Chin, "Miniature MOSFET radiation dosimeter probe," *Med. Phys.*, vol. 21, pp. 1721–1728, 1994.

[5] G. F. Knoll, *Radiation Detection and Measurement*. New York: Wiley, 1989.

[6] G. Polge, L. Dusseau, K. Idri, D. Plattard, J. Fesquet, J. Gasiot, and N. Iborra-Brassar, "Characterization of a 63 MeV proton beam with optically stimulated luminescent films," in *Proc. RADECS 2001 Conf.*, paper A-1, to be published.

[7] D. Plattard, L. Dusseau, J. R. Vaille, G. Ranchoux, G. Polge, J. Fesquet, R. Ecoffet, and J. Gasiot, "Characterization of an integrated sensor using optically stimulated luminescence for in flight dosimetry," in *Proc. RADECS 2001 Conf.*, paper A-2, to be published.

[8] B. O'Connell, C. Conneely, C. McCarthy, J. Doyle, W. Lane, and L. Adams, "Electrical performance and radiation sensitivity of stacked PMOS dosimeters under bulkbias control," *IEEE Trans. Nucl. Sci.*, vol. 45, pp. 2689–2694, Dec. 1998.

[9] [Online]. Available: www.nmrc.ie/projects/radfets/index.html

[10] S. M. Sze, *Physics of Semiconductor Devices*. New York: Wiley, 1981.

[11] G. Ristic, M. Pejovic, and A. Jaksic, "PMOS dosimetric transistors with two-layer gate oxide," *Sensors Actuators A*, vol. 63, pp. 129–134, 1997.

[12] P. J. McWhorter and P. S. Winokur, "Simple technique for separating the effects of interface traps and trapped-oxide charge in metal–oxide–semiconductor transistors," *Appl. Phys. Lett.*, vol. 48, pp. 133–135, 1986.

[13] G. Groeseneken, H. E. Maes, N. Beltran, and R. F. De Keersmaecker, "A reliable approach to charge-pumping measurements in MOS transistors," *IEEE Trans. Electron Devices*, vol. ED-31, pp. 42–53, 1984.

[14] B. M. Elliot, "The use of charge pumping currents to measure surface state densities in MOS transistors," *Solid-State Electron.*, vol. 19, pp. 241–247, 1976.

[15] D. M. Fleetwood, "Border traps in MOS devices," *IEEE Trans. Nucl. Sci.*, vol. 39, pp. 269–271, Apr. 1992.

[16] T. P. Ma and P. V. Dressendorfer, *Ionizing Radiation Effects in MOS Devices and Circuits*. New York: Wiley, 1989.

[17] D. M. Fleetwood, M. J. Johnson, T. L. Meisenheimer, P. S. Winokur, W. L. Warren, and S. C. Witczak, "$1/f$ noise, hydrogen transport and latent interface-trap buildup in irradiated MOS devices," *IEEE Trans. Nucl. Sci.*, vol. 44, pp. 1810–1817, Dec. 1997.

[18] K. F. Galloway, M. Gaitan, and T. J. Russell, "A simple model for separating interface and oxide charge effects in MOS device characteristics," *IEEE Trans. Nucl. Sci.*, vol. NS-31, pp. 1497–1501, Dec. 1984.

[19] D. M. Fleetwood, M. R. Shaneyfelt, J. R. Schwank, P. S. Winokur, and F. W. Sexton, "Theory and application of dual-transistor charge separation analysis," *IEEE Trans. Nucl. Sci.*, vol. 36, pp. 1816–1824, Dec. 1989.

[20] D. Zupac, K. F. Galloway, P. Khosropour, S. R. Anderson, and R. D. Schrimpf, "Separation of effects of oxide-trapped charge and interface-trapped charge on mobility in irradiated power VDMOSFET's," *IEEE Trans. Nucl. Sci.*, vol. 40, pp. 1307–1315, Dec. 1993.

[21] F. B. McLean and H. E. Boesch, Jr., "Time-dependent degradation of MOSFET channel mobility following pulsed irradiation," *IEEE Trans. Nucl. Sci.*, vol. 36, pp. 1772–1783, Dec. 1989.

[22] N. S. Saks, R. B. Klein, and D. L. Griscom, "Formation of interface traps in MOSFET's during annealing following low temperature irradiation," *IEEE Trans. Nucl. Sci.*, vol. 35, pp. 1234–1240, Dec. 1988.

[23] S. Dimitrijev and N. Stojadinovic, "Analysis of CMOS transistor instabilities," *Solid-State Electron.*, vol. 30, pp. 991–1003, 1987.

[24] A. J. Lelis, H. E. Boesch, Jr., T. R. Oldham, and F. B. McLean, "Reversibility of trapped hole annealing," *IEEE Trans. Nucl. Sci.*, vol. 35, pp. 1186–1191, Dec. 1988.

[25] A. J. Lelis, T. R. Oldham, H. E. Boesch, Jr., and F. B. McLean, "The nature of the trapped hole annealing process," *IEEE Trans. Nucl. Sci.*, vol. 36, pp. 1808–1815, Dec. 1989.

[26] A. J. Lelis and T. R. Oldham, "Time dependence of switching oxide traps," *IEEE Trans. Nucl. Sci.*, vol. 41, pp. 1835–1843, Dec. 1994.

[27] F. J. Feigl, W. B. Fowler, and K. L. Yip, "Oxygen vacancy model for the E_1' center in SiO_2," *Solid-State Commun.*, vol. 14, pp. 225–229, 1974.

[28] P. M. Lenahan and P. V. Dressendorfer, "Hole traps and trivalent silicon centers in metal/oxide/silicon devices," *J. Appl. Phys.*, vol. 55, pp. 3495–3499, 1984.

[29] D. M. Fleetwood, P. S. Winokur, R. A. Reber, Jr., T. L. Meisenheimer, J. R. Schwank, M. R. Shaneyfelt, and L. C. Riewe, "Effects of oxide traps, interface traps and border traps on metal–oxide–semiconductor devices," *J. Appl. Phys.*, vol. 73, pp. 5058–5074, 1993.

[30] V. S. Pershenkov, V. V. Belyakov, S. V. Cherepko, A. Y. Nikiforov, A. V. Sagoyan, V. N. Ulimov, and V. V. Emelianov, "Effect of electron traps on reversibility of annealing," *IEEE Trans. Nucl. Sci.*, vol. 42, pp. 1750–1757, Dec. 1995.

[31] V. S. Pershenkov, S. V. Cherepko, A. V. Sagoyan, V. V. Belyakov, V. N. Ulimov, V. V. Abramov, A. V. Shalnov, and V. I. Rusanovsky, "Proposed two-level acceptor–donor (AD) center and the nature of switching traps in irradiated MOS structures," *IEEE Trans. Nucl. Sci.*, vol. 43, pp. 2579–2586, Dec. 1996.

[32] D. M. Fleetwood, P. S. Winokur, L. C. Riewe, O. Flament, P. Paillet, and J. L. Leray, "The role of electron transport and trapping in MOS total-dose modeling," *IEEE Trans. Nucl. Sci.*, vol. 46, pp. 1519–1525, Dec. 1999.

[33] M. Walters and A. Reisman, "Radiation-induced neutral electron trap generation in electrically biased insulated gate filed effect transistor gate insulators," *J. Electrochem. Soc.*, vol. 138, pp. 2756–2762, 1991.

[34] P. J. McWhorter, S. L. Miller, and W. M. Miller, "Modeling the anneal of radiation-induced trapped holes in a varying thermal environment," *IEEE Trans. Nucl. Sci.*, vol. 37, pp. 1682–1689, Dec. 1990.

[35] D. B. Brown and N. S. Saks, "Time dependence of radiation-induced interface trap formation in metal–oxide–semiconductor devices as a function of oxide thickness and applied field," *J. Appl. Phys.*, vol. 70, pp. 3734–3747, 1991.

[36] R. E. Stahlbush, A. H. Edwards, D. L. Griscom, and B. J. Mrstik, "Post-irradiation cracking of H_2 and formation of interface states in irradiated metal–oxide–semiconductor field-effect transistors," *J. Appl. Phys.*, vol. 73, pp. 658–667, 1993.

[37] P. M. Lenahan, J. J. Mele, J. F. Conley, Jr., R. K. Lowry, and D. Woodbury, "Predicting radiation response from process parameters: Verification of a physically based predictive model," *IEEE Trans. Nucl. Sci.*, vol. 46, pp. 1534–1543, Dec. 1999.

[38] J. R. Schwank and D. M. Fleetwood, "Effect of post-oxidation anneal temperature on radiation-induced charge trapping in metal–oxide–semiconductor devices," *Appl. Phys. Lett.*, vol. 53, pp. 770–772, 1988.

[39] W. L. Warren, D. M. Fleetwood, M. R. Shaneyflet, J. R. Schwank, P. S. Winokur, R. A. B. Devine, and D. Mathiot, "Links between oxide, interface, and border traps in high-temperature annealed Si/SiO_2 systems," *Appl. Phys. Lett.*, vol. 64, pp. 3452–3454, 1994.

[40] T. R. Oldham, A. J. Lelis, and F. B. McLean, "Spatial dependence of trapped holes determined from tunneling analysis and measured annealing," *IEEE Trans. Nucl. Sci.*, vol. NS-33, pp. 1203–1209, Dec. 1986.

[41] R. K. Freitag, E. A. Burke, C. M. Dozier, and D. B. Brown, "The development of nonuniform deposition of holes in gate oxides," *IEEE Trans. Nucl. Sci.*, vol. 35, pp. 1203–1207, Dec. 1988.

[42] Z. Savic, B. Radjenovic, M. Pejovic, and N. Stojadinovic, "The contribution of border traps to threshold voltage shift in pMOS dosimetric transistors," *IEEE Trans. Nucl. Sci.*, vol. 42, pp. 1445–1454, Aug. 1995.

[43] R. C. Hughes, W. R. Dawes, Jr., W. Meyer, and S. W. Yoon, "Dual dielectric silicon metal–oxide–semiconductor field-effect transistors as radiation sensors," *J. Appl. Phys.*, vol. 65, pp. 1972–1976, 1989.

[44] J. R. Schwank, S. B. Boeske, D. E. Beutler, D. J. Moreno, and M. R. Shaneyfelt, "A dose rate independent PMOS dosimeter for space applications," *IEEE Trans. Nucl. Sci.*, vol. 43, pp. 2671–2678, Dec. 1996.